

# A comparative investigation of methods for protein immobilization on self-assembled monolayers using glutaraldehyde, carbodiimide, and anhydride reagents

Robert E. Ducker, Matthew T. Montague, and Graham J. Leggett<sup>a)</sup>

Department of Chemistry, University of Sheffield, Brook Hill, Sheffield S3 7HF, United Kingdom

(Received 16 May 2008; accepted 1 August 2008; published 17 September 2008)

Three different approaches to the immobilization of proteins at surfaces have been compared. All rely on the creation of surface groups that bind primary amines on lysine residues. Carboxylic acid terminated self-assembled monolayers (SAMs) have been activated using a water soluble carbodiimide to yield an active ester functionalized surface and with trifluoroacetic anhydride to yield a surface anhydride, and amine terminated SAMs have been activated using glutaraldehyde. Although the degree of surface derivatization by *n*-alkylamines was greater using the carbodiimide and anhydride methods under anhydrous conditions, the glutaraldehyde activation of amine terminated SAMs yielded significantly greater attachment of streptavidin than is achieved using either of the other methods. This is attributed to the susceptibility to hydrolysis of the active species formed by activation of the carboxylic acid terminated monolayers. Patterned protein structures may be formed by using both glutaraldehyde activation of amine terminated thiols and carbodiimide activation of carboxylic acid terminated thiols, in conjunction with selective photo-oxidation of oligo(ethylene glycol) terminated SAMs. © 2008 American Vacuum Society.  
[DOI: 10.1116/1.2976451]

## I. INTRODUCTION

There is a growing interest in the fabrication of biochips for applications in sensing and biomolecular analysis.<sup>1</sup> In addition to a suitable signal transduction mechanism, there are typically two other important requirements. A means of controlling the interactions between biological entities and the solid surface presented by the transducing element (involving both the selective attachment of functional species to solid surfaces and also the inhibition of nonspecific binding) is ubiquitous. Since the rapid growth of demand for high-throughput systems for genomics, proteomics, and glycomics, a means of controlling the spatial organization of those interactions has additionally become important. Such spatial control of biological organization is also a necessary requirement for many fundamental studies of interfacial biological phenomena. Following the groundbreaking works of Curtis and Forrester,<sup>2,3</sup> Curtis and McMurray,<sup>4</sup> Whitesides and co-workers,<sup>5-7</sup> and Brunette,<sup>8</sup> there has been a rapid growth in activity based on the exploration of cellular responses to topographical,<sup>9-11</sup> chemical,<sup>5,6,12</sup> mechanical,<sup>7,13-15</sup> and other cues on small length scales. While early work in this area explored cellular interactions with micrometer-scale structures, some recent studies have begun to explore the influence of nanometer-scale assemblies on the cellular behavior. Notable examples include the work of Spatz and co-workers<sup>16,17</sup> on the exploitation of micelle-based self-assembly techniques to fabricate ligands for cell receptors with dimensions of a few tens of nanometers and the work of

Lee *et al.*<sup>18</sup> utilizing dip-pen nanolithography to pattern cell adhesive molecules to form structures with dimensions of approximately 200 nm.

Protein patterning requires two elements. First, a means of inhibiting the attachment of proteins to the majority of the surface, and second, some means of securely anchoring the protein at specific desired locations. The tendency of proteins to adsorb irreversibly onto most surfaces is a major problem. In the extreme, nonspecific adsorption may render it impossible to read data from a chip; more commonly, however, it leads to a reduction in the signal-to-noise ratio, reducing the sensitivity of the system. The “gold standard” protein-resistant materials are self-assembled monolayers (SAMs) of oligo(ethylene glycol) (OEG) terminated alkylthiols<sup>19,20</sup> (although it should be noted that there is a growing number of systems that exhibit similar performance, including polymer brushes formed by graft polymerization and surface initiated atom-transfer radical polymerization<sup>21-23</sup> and plasma-polymerized tetraglyme films<sup>24,25</sup>). The principal objective of this paper is to compare the efficacy of three different methods for immobilizing a protein molecule to the surface: activation of surface amines with glutaraldehyde (GA) to form an aldehyde-functionalized surface,<sup>26</sup> formation of an intramonomer anhydride from a carboxylic acid,<sup>27</sup> and formation of an active ester from a carboxylic acid.<sup>28</sup> All involve coupling of a reactive surface-bound functional group to a free amine group (on a lysine residue) in the protein molecule. It should be noted that while the present study is focused on the immobilization of proteins, the methods studied are of widespread applicability, being used to immobilize other biomolecules (for example oligonucleotides) and other types of functional object (for example, nanoparticles<sup>29</sup>). It has been found that glutaraldehyde activation of an amine

<sup>a)</sup>Electronic mail: graham.leggett@shef.ac.uk

terminated SAM yields significantly more protein attachment than is observed for either active ester or anhydride derivatized surfaces. Because proteins often contain a number of lysine residues, which may be distributed widely through the protein structure, these methods do not facilitate site-specific immobilization, except in unusual cases such as light harvesting complex 2 (LH2) from *R. Sphaeroides*, in which the lysine residues are all found on the cytoplasmic face of the protein, which means that active ester methods yield immobilization with controlled orientation.<sup>30</sup> However, the active ester method has nevertheless been very widely used. Streptavidin attachment has been widely utilized, in conjunction with such approaches, because the availability of multiple binding sites for biotin means that even though control of protein orientation is not possible, there remains a high probability that a biotinylated antibody will be bound. If the biotinylation is site-specific, then protein orientation can be controlled indirectly.

## II. EXPERIMENTAL SECTION

### A. SAM preparation

Mercaptoundecanoic acid ( $C_{10}COOH$ ), dodecanthiol ( $C_{11}CH_3$ ), and lysine were purchased from Sigma Chemical Co. (Poole, UK).  $C_{10}COOH$  was recrystallized from hexane before use. Aminoundecanethiol hydrochloride [ $HS(CH_2)_{11}NH_3^+Cl^-$  hereafter  $C_{11}NH_3$ ] was purchased from NBS Biologicals (Cambridge, UK). (1-mercaptoundec-11-yl)tri(ethylene glycol) [ $C_{11}(OEG)_3$ ] was synthesized according to a method previously published by Pale-Grosdemange *et al.*<sup>20</sup> Glassware was cleaned using piranha solution (a 7:3 mixture of 30% hydrogen peroxide and concentrated sulfuric acid), rinsed with copious quantities of de-ionized water, and dried overnight in an oven prior to use. Care must be exercised when using piranha solution, which reacts violently with organic materials.

SAMs were prepared by immersing freshly deposited gold-coated chromium-primed glass microscope slides (Chance Proper no. 2 thickness, size of  $22 \times 64$  mm<sup>2</sup>) in 1 mM solutions of the appropriate thiol in ethanol. The thickness of the gold film was 50 nm, and the chromium layer was 2–3 nm thick. Ethanol was thoroughly degassed using nitrogen prior to use. Samples were cut into the required shape, washed with ethanol, and dried under a stream of nitrogen.

### B. Anhydrous coupling reactions

Anhydrous surface reactions were prepared using a Schlenk line. Anhydrous (99.9%, <50 ppm water) *N,N*-dimethylformamide (DMF) (Acros Organics, Loughborough, UK) was used as the solvent. Samples were placed in vials sealed with rubber septa. The vials were dried before use in an oven, and samples inserted as soon as the vials were cooled. The samples were allowed to cool under vacuum. Following insertion of the sample, the vial was sealed, then evacuated, and then filled with nitrogen. All reagents were also handled in a nitrogen atmosphere. The reaction mixtures were transferred to the vial containing the

sample via a cannula. After completion of the reaction, the sample was rinsed with chloroform and dried in a stream of nitrogen gas.

To prepare active ester derivatives of  $C_{10}COOH$ , a method adapted from that of Patel *et al.* was used.<sup>28</sup> A solution of 100 mM 1-ethyl-3,3-dimethyl carbodiimide (EDC) (Sigma) and 100 mM *N*-hydroxysuccinimide (NHS) (Sigma) was prepared in dimethylformamide (DMF) and sonicated. The sample was immersed in this solution for 20 min with the lid of the vial replaced.

Anhydride surfaces were formed by the reaction of trifluoroacetic anhydride (TFAA) with a  $C_{10}COOH$  monolayer, following the method of Yan *et al.*<sup>27</sup> A solution of 100 mM triethylamine and 100 mM TFAA in DMF was prepared. The sample was then immediately immersed in the solution for 20 min, with the lid loosely placed on the vial.

Aldehyde terminated monolayers were prepared from  $C_{11}NH_2$  monolayers by reaction with GA (Sigma). A 25% solution of GA was first diluted to 12.5% with de-ionized (resistivity of 18.2 M $\Omega$ ) water. The sample was immersed in the solution for 20 min, with the lid of the vial replaced.

Lysine films were formed by first activating amine terminated monolayers with GA as described above. The activated monolayers were then immersed in a 10 mM solution of lysine in H<sub>2</sub>O for 20 min.

### C. Undecylamine derivatization

The undecylamine derivatization was carried out by first activating the samples using the methods described above and then transferring the samples to a 10 mM solution of undecylamine in ethanol for 20 min.

### D. Protein binding

Unless otherwise stated, all protein solutions were prepared with a concentration of 5  $\mu\text{g ml}^{-1}$  in 100 mM phosphate buffered saline solution (PBS), pH 7.8.

### E. Characterization

Sessile drop contact angle measurements were made using a Rame–Hart model 100–00 contact angle goniometer. Surface plasmon resonance (SPR) spectroscopy was carried out using the Biacore 3000 (Biacore AB, Uppsala, Sweden). All protein concentrations were 100  $\mu\text{g ml}^{-1}$  run in a buffer of PBS at a constant flow rate of 20  $\mu\text{l s}^{-1}$ . A baseline was acquired for 10 min allowing the system to equilibrate. Then 200  $\mu\text{l}$  of protein solution was injected into the system over a period of 10 min with a further flow of buffer for 10 min. The nonspecifically adsorbed protein was washed from the surface with sodium dodecyl sulfate (SDS) (0.01% w/w) and allowed to equilibrate for a further 2 min. If required, the antibody was then introduced into the system before the SDS wash, repeating the same 10 min injection followed by 10 min of buffer flow.

X-ray photoelectron spectroscopy (XPS) was carried out using a Kratos Analytical Axis Ultra X-ray Photoelectron Spectrometer, fitted with a delay line detector (Kratos Ana-

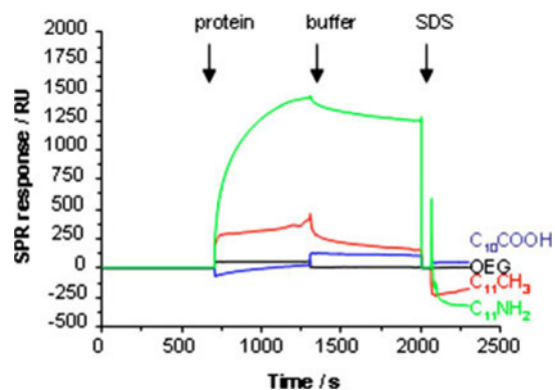


FIG. 1. SPR data showing the change in the response as a function of time for a variety of different surfaces following injection of streptavidin, followed by buffer, and finally SDS.

lytical, Manchester, UK). The x-ray source was an Al  $K\alpha$  ( $h\nu=1486.6$  eV) with an anode current of 6.0 mA and an anode voltage of 15 kV with the resulting x-ray power of 90 W. Wide scans were collected at 160 eV and narrow scans at 80 eV. Samples were prepared as above and cut into 5  $\times$  5 mm<sup>2</sup> squares.

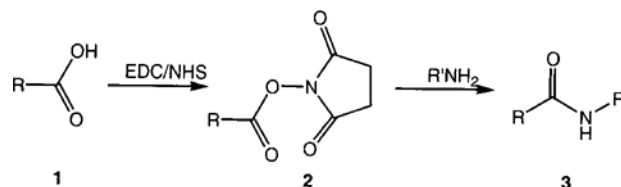
## F. Patterning

Micrometer-scale photopatterning of SAMs was carried out by exposing the sample through a chromium electron microscopy grid to light from with a Coherent Innova 300C FreD (frequency-doubled) argon ion laser (Coherent Ltd., Ely, UK). The fundamental emission wavelength was 488 nm; UV wavelengths were obtained by doubling the frequency of the 488 nm line using Brewster-cut beta-barium borate crystal, yielding a wavelength of 244 nm with a typical power of 100 mW.

## III. RESULTS AND DISCUSSION

### A. Physical adsorption

Streptavidin was adsorbed onto methyl, amine, carboxylic acid, and OEG terminated SAMs. The data are shown in Fig. 1. For the OEG terminated SAM, an initial perturbation in the SPR signal was observed following injection of the protein solution, but after injecting buffer solution, the SPR signal returned to its initial value. These data indicated that the OEG terminated SAM was resistant to streptavidin adsorption, in agreement with the previously published literature. All of the other materials exhibited significant amounts of protein adsorption, even after rinsing with buffer, in the order of  $C_{11}NH_2 > C_{10}COOH > C_{11}CH_3$ . To test the reversibility of adsorption, the samples were washed with SDS. The detergent was found to elute the streptavidin from the surface, suggesting that it was capable of disrupting nonspecific interactions between streptavidin and all of the SAMs studied here.



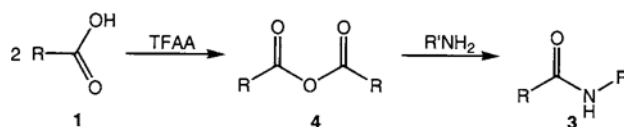
SCHEME 1. Activation of a carboxylic acid terminated monolayer using EDC/NHS, followed by reaction with an amine to yield an amide linkage.

### B. Covalent attachment mechanisms

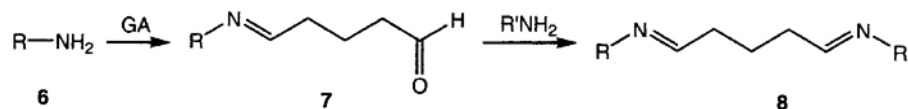
Three strategies for the covalent attachment of proteins were compared. All relied on the creation of surface functional groups that bind amine groups; lysine residues contain free amine groups and such strategies are attractive because they are potentially generically applicable. The first strategy, based on the conversion of a carboxylic acid group (1) into an *N*-hydroxysuccinimide ester (2) by exposure of a suitable SAM to a solution of a 1-ethyl-3,3-dimethyl carbodiimide and *N*-hydroxysuccinimide (EDC/NHS), has been widely used for surface immobilization of proteins (Scheme 1). The active ester is susceptible to nucleophilic attack by an amine group, leading to the formation of an amide bond linking the protein to the monolayer (3). Generally, in literature reports, the activation is carried out in aqueous conditions. However, the active ester is susceptible to hydrolysis.<sup>31</sup> In the present work, therefore, we used DMF as the solvent for the activation step. This was found to yield more reproducible data and also to yield better surface functionalization, irrespective of whether the subsequent immobilization step was aqueous (for proteins) or anhydrous (for amines in model studies).

The second strategy (Scheme 2) was also based on the formation of an amide bond from the protein to the surface. Following the method of Yan *et al.*,<sup>27</sup> carboxylic acid terminated SAMs were activated by exposure to a solution of TFAA, yielding a surface anhydride species (4). This activated surface is then transferred to the protein solution with a free amine on the protein immobilizing it at the surface.

Finally, GA was used to activate amine terminated SAMs (Scheme 3). GA is readily available and widely used for the preparation of biological specimens for microscopy (for example, many specimens are “fixed” by cross-linking with GA prior to microscopical investigation). GA is a bifunctional molecule that contains two aldehyde groups separated by a short alkyl chain. It will thus react with an amine functionalized surface (6) through one end to form an imine bond, yielding an aldehyde-functionalized surface (7) which may, in turn, react with an amine to form an imine (8).<sup>26</sup> The



SCHEME 2. Activation of a carboxylic acid terminated monolayer using TFAA, followed by reaction with an amine to yield an amide linkage.



SCHEME 3. Reaction of GA with an amine terminated monolayer to yield an aldehyde functionalized surface that may subsequently react with an amine to form an imine linkage.

imine may be converted into an amide but this was not explored in the present study. It thus offers a simple route to the immobilization of proteins, but has, thus far, been comparatively little used for surface functionalization.

Initially, these three methods were tested using a model system to facilitate comparison of binding under well-controlled conditions. An amine, *n*-undecylamine, was coupled to the surface, and the change in the contact angle is measured. All of the surfaces used were hydrophilic, with contact angles less than  $20^\circ$  in agreement with the previously published results. Figure 2 shows measurements of the con-

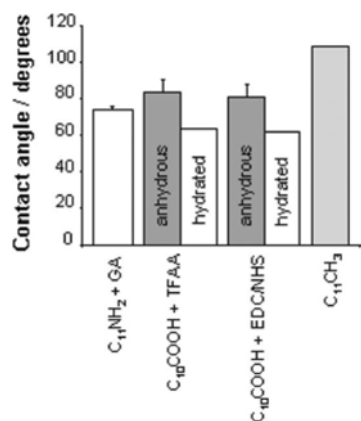


FIG. 2. Contact angles of surfaces following activation under different conditions and reaction with undecylamine. For reference, the contact angle is also shown for a SAM of dodecanthiol.

tact angles of all of the surfaces following the derivatization reaction. As a point of reference, the contact angle of a SAM of dodecanthiol ( $C_{11}CH_3$ ) is also shown, as an indication of the value expected for a close-packed monolayer of hydrophobic molecules. Two sets of data are shown for the EDC/NHS and TFAA methods: “anhydrous” data (gray bars) refer to experiments in which the surface activation process was conducted under rigorously anhydrous conditions (using a Schlenk line to maintain a nitrogen atmosphere), while the other data (white bars) refer to experiments in which no special care was taken to exclude the ingress of water into the reaction system.

It can be seen that both the anhydrous derivatization conditions yield very similar contact angles: the contact angle rises to  $81^\circ$  and  $83^\circ$  for the EDC/NHS and TFAA methods, respectively; hence, within experimental error, the results are indistinguishable. In both cases, the contact angle is less than that of a  $C_{11}CH_3$  monolayer, indicating that derivatization is not complete.

To validate the use of contact angles to measure the extent of surface reactions, comparative measurements were made by XPS for the anhydrous coupling reactions (Fig. 3). The C 1s XPS spectrum of  $C_{10}COOH$  exhibits a characteristic peak at 285.0 eV due to the aliphatic chain and a peak due to the carboxylic acid carbon at 289.3 eV. The C 1s spectrum following activation with EDC/NHS is more complex because of contributions from the active ester functionality. Upon reaction with undecylamine, the spectrum becomes simpler, exhibiting three principal components—the aliphatic

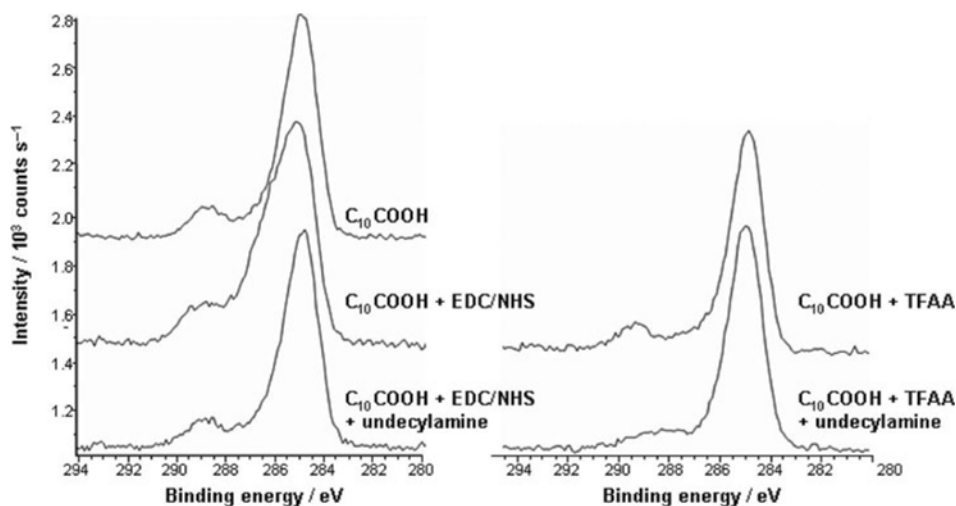


FIG. 3. C 1s XPS spectra for  $C_{10}COOH$  (top left) and for  $C_{10}COOH$  following activation with EDC/NHS (left middle and lower) and TFAA (right hand side) and derivatization with undecylamine (bottom row).

TABLE I. Elemental compositions for amine and carboxylic acid terminated SAMs following derivatization with GA, TFAA, and EDC/NHS, and subsequent reaction with undecylamine.

System	C	N	N/C	N/C calc.
AUT	35.6	4.6	0.13	0.091
AUT/GA activation	48.4	3.9	0.08	0.063
AUT/GA activation + undecylamine	46.3	4.7	0.10	0.074
MUA	57.6	0	0	0
MUA/TFAA activation	47.3	0	0	0
MUA/EDC/NHS activation	54.2	6.3	0.12	0.067
MUA/TFAA activation + undecylamine	52.9	2.2	0.04	0.045
MUA/EDC/NHS activation + undecylamine	50.2	1.6	0.03	0.045

carbon atoms in the alkyl chain, an amide component at 287.9 eV, and a component at 289.3 eV due to unreacted carboxylic acid groups. The extent of reaction may readily be estimated from the elemental composition (Table I). The N/C ratio is calculated to be 0.045 for 100% conversion of carboxylic acids to amides. The measured value was 0.030. While the product is long enough for there to be substantial attenuation of the signal from the lower alkyl chain, the nitrogen atom is situated between two chains of 11 carbon atoms in length, and so attenuation of the N 1s signal by the upper chain should be balanced by attenuation of the C 1s signal from the lower chain. Hence, while the data suggest significant derivatization of the activated surface by the amine, they confirm the prediction from the contact angle data that the reaction does not yield 100% derivatization.

Activation of the C<sub>10</sub>COOH monolayer with TFAA yields a spectrum very similar to that obtained for the unreacted carboxylic acid because the product of the derivatization contains aliphatic carbon chains and carboxylate carbon atoms. There is no peak for CF<sub>3</sub> which would be expected at approximately 292.0 eV because the anhydride is formed via interchain reaction within the monolayer. The reaction of the anhydride surface with undecylamine yields an additional component corresponding to the resulting amide. Again, the N/C ratio (0.04) is substantial but indicative of incomplete derivatization, in agreement with the contact angle data.

The contact angle measured following derivatization with GA and attachment of undecylamine was 76°, slightly less than the angle measured using the anhydrous EDC/NHS and TFAA methods but not substantially so. However, GA is not readily available in anhydrous form, being typically supplied in aqueous solution. The contact angle obtained using the GA activation step was significantly greater than that obtained using EDC/NHS and TFAA activation when steps were not taken to maintain rigorously anhydrous conditions; the latter methods yield contact angles of only 62° and 63°, respectively, indicating very much lower levels of attachment of the amine and suggesting that these methods are comparatively ineffective under conditions where the amount of moisture in the reaction system is not controlled.

Measurements were also made by XPS for the GA activated surfaces. The N 1s XPS spectrum of C<sub>11</sub>NH<sub>2</sub> (Fig. 4) exhibited a single peak at 401.0 eV corresponding to the

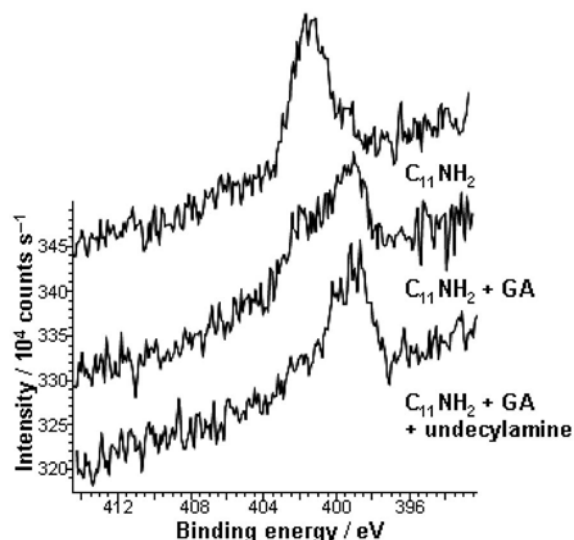


FIG. 4. N 1s XPS spectra for (top) C<sub>11</sub>NH<sub>2</sub>; (center) C<sub>11</sub>NH<sub>2</sub> following activation with GA; (bottom) following incubation of the activated surface with a solution of undecylamine.

terminal amine group. Upon the addition of GA, a second peak was observed, which are consistent with the formation of an imine. The addition of undecylamine yields a spectrum containing two peaks with binding energies of 402.0 and 399.1 eV, corresponding to amine and imine peaks, respectively. Although the extent of reaction is significant, a shoulder persists at the high binding energy side of the peak, indicating that some unreacted amine remains. Moreover, the significance of this component is increased by the fact that two imine nitrogens are attributable to each immobilized undecylamine molecule, whereas each unreacted adsorbate has only one amine nitrogen. From analysis of the relative areas of the two components, following deconvolution, it was determined that the extent of derivatization by undecylamine was 52%.

The anhydrous method is clearly not applicable to the immobilization of a protein, and for coupling reactions that must proceed in aqueous solutions, such as those involving proteins, the GA method is clearly the one that facilitates the highest yield.

### C. Protein attachment

The coupling of proteins to the surface was characterized using SPR. Figure 5 shows the variation in the SPR response with time for three activated surfaces following exposure to a solution of streptavidin. The initial rise in the SPR response was very similar for TFAA and EDC/NHS activated surfaces, and for both surfaces, the SPR response dropped by approximately one-third following subsequent rinsing of the samples with buffer solution. SDS was passed through the SPR cell in order to elute reversibly adsorbed protein; the fraction remaining after exposure to SDS was irreversibly bound and likely to consist mainly of covalently bound protein molecules. After the introduction of SDS, the SPR response reached a value somewhat smaller than the initial maximum

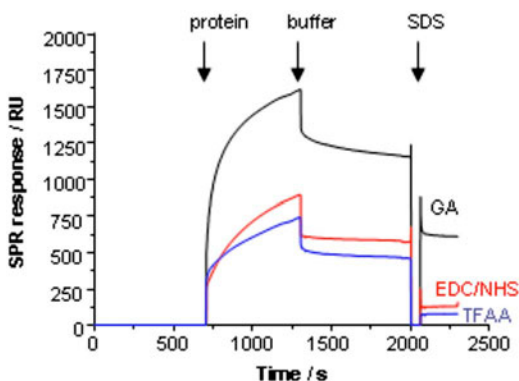


FIG. 5. SPR data comparing the binding of streptavidin by GA, EDC/NHS, and TFAA activated SAMs.

value reached following the introduction of the protein (approximately 15% in the case of EDC/NHS and approximately 10% in the case of TFAA).

The behavior was markedly different for GA activated surfaces. The initial rise in SPR response following the introduction of the streptavidin solution was approximately twice that of the TFAA activated surface (1625 and 750 response units (RU), respectively) and somewhat more than that observed for the EDC/NHS-activated surface (880 RU). After rinsing with buffer and then SDS, the signal measured for the GA activated surface remained significantly larger than that measured for either of the other two (620 RU compared to 125 for the EDC/NHS activated surface). These data strongly suggest that under the conditions used to immobilize the protein (i.e., aqueous buffer) the efficiency of coupling to the GA surface is significantly greater than the efficiency of coupling to the other activated surfaces.

To test whether this difference in binding was accompanied by a corresponding difference in the biological activity of the immobilized protein film, streptavidin was bound to EDC/NHS and GA activated surfaces and then exposed to biotinylated bovine serum albumin (BSA). Figure 6 shows the resulting SPR data. In agreement with the data in Fig. 5, the amount of streptavidin binding to the GA activated surface was approximately twice that binding to the EDC/NHS activated surface (1650 and 800 RU, respectively), and the amount of biotinylated BSA bound was also larger (2500 and 1175 RU for GA and EDC-NHS activated surfaces, respectively). The increase in the amount of biotinylated BSA on the GA activated surface was approximately proportional to the increase in the amount of immobilized streptavidin, suggesting that the two coupling schemes yield a similar degree of activity in the immobilized protein probably because the protein is randomly oriented in both cases; the principal difference is thus that substantially more streptavidin is coupled to the GA activated surface.

The covalent attachment of BSA was studied for comparative purposes. The data are shown in Fig. 7. In this case, the initial rise in the SPR response following injection of the protein solution, approximately 2000 RU, was very similar for both surface activation steps. However, following rinsing

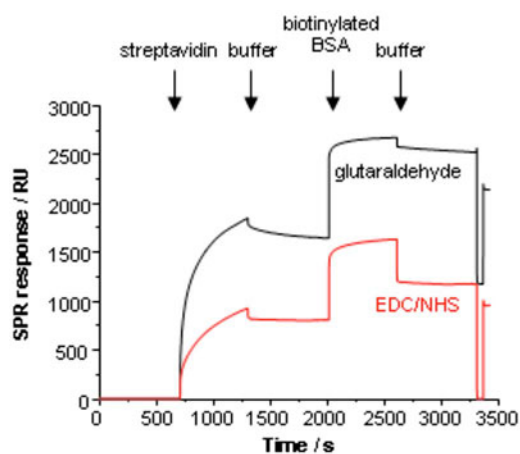


FIG. 6. The variation in the SPR response during coupling of streptavidin to EDC and GA activated surfaces, followed by exposure to biotinylated BSA.

with buffer, and then elution of noncovalently bound protein using SDS, it was found that more protein remained on the GA activated surface than remained on the EDC/NHS activated surface, with the SPR responses being 1180 and 720, respectively. The difference was slightly smaller than what was measured for streptavidin immobilization but nevertheless substantial.

#### D. Photopatterning

Micron-scale patterns were formed by photopatterning to confirm the compatibility of both GA and EDC/NHS activation with spatial control of protein attachment. Exposure of SAMs to UV light causes photo-oxidation of the head group,<sup>32</sup> leading to the formation of weakly bound alkylsulfonate species that are readily displaced by a second solution-phase thiol to yield a pattern. Monolayers of  $C_{11}(\text{OEG})_3$  were exposed to UV light (244 nm) through a mask. Following exposure, the samples were immersed in either  $C_{11}\text{NH}_2$  or  $C_{10}\text{COOH}$ . The resulting patterns consisted of contrasting polar regions. Micropatterned samples were activated using either GA [ $C_{11}(\text{OEG})_3/C_{11}\text{NH}_2$  patterns] or

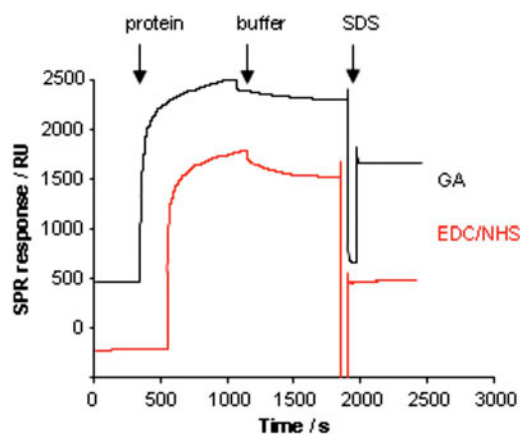


FIG. 7. The variation in the SPR response during coupling of BSA to EDC and GA activated surfaces.

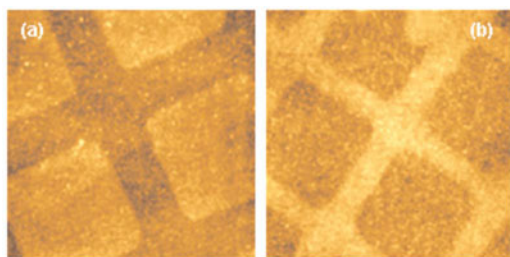


FIG. 8. Tapping mode height images of photopatterned SAMs: (a) IgG coupled to GA activated  $C_{11}(\text{OEG})_3/C_{11}\text{NH}_2$  patterns ( $37.6 \times 37.6 \mu\text{m}^2$ ). (b) IgG coupled to EDC/NHS-activated  $C_{11}(\text{OEG})_3/C_{10}\text{COOH}$  patterns ( $50.0 \times 50.0 \mu\text{m}^2$ ).

EDC/NHS ( $C_{11}(\text{OEG})_3/C_{10}\text{COOH}$  patterns), and then immersed in solutions of immunoglobulin (IgG). The resulting patterns were imaged using tapping mode atomic force microscope (Fig. 8). In Fig. 8(a), the square regions contain the immobilized protein and the bars consist of  $C_{11}(\text{OEG})_3$ , while in Fig. 6(b), the square regions are composed of  $C_{11}(\text{OEG})_3$ , while the bars are occupied by immobilized protein. In both cases, despite the difference in the reactivity of the activated surfaces toward proteins, the topographical contrast was sufficiently clear for the patterns to be clearly evident.

#### IV. CONCLUSIONS

Carboxylic acid terminated SAMs may be activated using EDC/NHS or TFAA to yield surfaces that are reactive toward amines. For *n*-alkylamines, the degree of surface derivatization is much greater when the attachment reaction is carried out under rigorously anhydrous conditions. When no efforts are made to eliminate water from the reaction system, the degree of derivatization is significantly smaller than that achieved following reaction with amine terminated SAMs that have been activated using GA. GA activation of amine terminated SAMs yields substantially more attachment of streptavidin than is achieved using either the EDC/NHS or TFAA activation of carboxylic acid terminated SAMs. GA activation of amine terminated SAMs is much simpler than either of the other methods and appears to offer a useful general method of protein attachment. Both GA activation and EDC/NHS activation are compatible with the formation of patterned protein structures by selective photo-oxidation of OEG terminated SAMs.

#### ACKNOWLEDGMENTS

The authors thank Dr. T. J. Whittle and Mr. N. P. Reynolds for assistance with the acquisition of XPS spectra. R.E.D. and M.T.M. thank the Biotechnology and Biological

Sciences Research Council (BBSRC) for Research Committee Studentships. G.J.L. thanks the EPSRC-GB and the RSC Analytical Chemistry Trust Fund for their support. The authors thank BBSRC (Grant No. EGM17711) for financial support.

- <sup>1</sup>J. J. Davis, D. A. Morgan, C. L. Wrathmell, D. N. Axford, J. Zhao, and N. Wang, *J. Mater. Chem.* **15**, 2160 (2005).
- <sup>2</sup>A. S. G. Curtis and J. V. Forrester, *J. Cell. Sci.* **71**, 17 (1986).
- <sup>3</sup>A. S. G. Curtis, J. V. Forrester, and P. Clark, *J. Cell. Sci.* **86**, 9 (1986).
- <sup>4</sup>A. S. G. Curtis and H. McMurray, *J. Cell. Sci.* **86**, 25 (1986).
- <sup>5</sup>G. P. Lopez, H. A. Biebuyck, R. Haerter, A. Kumar, and G. M. Whitesides, *J. Am. Chem. Soc.* **115**, 10774 (1993).
- <sup>6</sup>R. Singhvi, A. Kumar, G. P. Lopez, G. N. Stephanopoulos, D. I. C. Wang, G. M. Whitesides, and D. E. Ingber, *Science* **264**, 696 (1994).
- <sup>7</sup>C. S. Chen, M. Mrksich, S. Huang, G. M. Whitesides, and D. E. Ingber, *Science* **276**, 1425 (1997).
- <sup>8</sup>D. M. Brunette, *Exp. Cell Res.* **164**, 11 (1986).
- <sup>9</sup>B. Chehroudi, T. R. L. Gould, and D. M. Brunette, *J. Biomed. Mater. Res.* **24**, 1203 (1990).
- <sup>10</sup>B. Chehroudi, T. R. L. Gould, and D. M. Brunette, *J. Biomed. Mater. Res.* **25**, 387 (1991).
- <sup>11</sup>P. Clark, P. Connolly, A. S. G. Curtis, J. A. T. Dow, and C. D. W. Wilkinson, *J. Cell. Sci.* **99**, 73 (1991).
- <sup>12</sup>C. A. Scotchford, E. Cooper, S. Downes, and G. J. Leggett, *J. Biomed. Mater. Res.* **41**, 431 (1998).
- <sup>13</sup>C. H. Thomas, J.-B. Lhoest, D. G. Castner, C. D. MacFarland, and K. E. Healy, *J. Biomech. Eng.* **121**, 40 (1999).
- <sup>14</sup>S. Huang and D. E. Ingber, *Exp. Cell Res.* **261**, 91 (2000).
- <sup>15</sup>C. H. Thomas, J. H. Collier, C. S. Sfeir, and K. E. Healy, *Proc. Natl. Acad. Sci. U.S.A.* **99**, 1972 (2002).
- <sup>16</sup>E. A. Cavalcanti-Adam, T. Volberg, A. Micoulet, H. Kessler, B. Geiger, and J. P. Spatz, *Biophys. J.* **92**, 2964 (2007).
- <sup>17</sup>A. E. Calvacanti-Adam, A. Micoulet, J. Blümmel, J. Auernheimer, H. Kessler, and J. P. Spatz, *Eur. J. Cell Biol.* **85**, 219 (2006).
- <sup>18</sup>K.-B. Lee, S.-J. Park, C. A. Mirkin, J. C. Smith, and M. Mrksich, *Science* **295**, 1702 (2002).
- <sup>19</sup>K. L. Prime and G. M. Whitesides, *Science* **252**, 1164 (1991).
- <sup>20</sup>C. Pale-Grosdemange, E. S. Simon, K. L. Prime, and G. M. Whitesides, *J. Am. Chem. Soc.* **113**, 12 (1991).
- <sup>21</sup>H. Ma, D. Li, X. Sheng, B. Zhao, and A. Chilkoti, *Langmuir* **22**, 3751 (2006).
- <sup>22</sup>H. Ma, M. Textor, R. L. Clark, and A. Chilkoti, *BioInterphases* **1**, 35 (2006).
- <sup>23</sup>H. Ma, M. Wells, T. P. Beebe, Jr., and A. Chilkoti, *Adv. Funct. Mater.* **16**, 640 (2006).
- <sup>24</sup>G. P. López, B. D. Ratner, C. Tidwell, C. Haycox, R. Rapoza, and T. Horbett, *J. Biomed. Mater. Res.* **26**, 415 (1992).
- <sup>25</sup>M. Shen, M. Wagner, D. Castner, B. Ratner, and T. Horbett, *Langmuir* **19**, 1692 (2003).
- <sup>26</sup>H. Wang, D. G. Castner, B. D. Ratner, and S. Jiang, *Langmuir* **20**, 1877 (2004).
- <sup>27</sup>L. Yan, C. Marzolin, A. Terfort, and G. M. Whitesides, *Langmuir* **13**, 6704 (1997).
- <sup>28</sup>N. Patel, M. C. Davies, M. Hartshorne, R. J. Heaton, C. J. Roberts, S. J. Tendler, and P. M. Williams, *Langmuir* **13**, 6485 (1997).
- <sup>29</sup>S. Sun, M. Montague, K. Critchley, M.-S. Chen, W. J. Dressick, S. D. Evans, and G. J. Leggett, *Nano Lett.* **6**, 29 (2006).
- <sup>30</sup>N. P. Reynolds *et al.*, *J. Am. Chem. Soc.* **129**, 14625 (2007).
- <sup>31</sup>F. Cheng, L. J. Gamble, D. W. Grainger, and D. G. Castner, *Anal. Chem.* **79**, 8781 (2007).
- <sup>32</sup>G. J. Leggett, *Chem. Soc. Rev.* **35**, 1150 (2006).